Received: 24 November 2017 | Revised: 18 May 2018 | Accepted: 6 June 2018

DOI: 10.1002/poc.3873

RESEARCH ARTICLE

WILEY Journal of Physical Organic Chemistry

Some novel nanostructure Schiff base compounds: Antimicrobial and thermal behaviors

S. Khani[1] | M. Montazerozohori[1] | R. Naghiha[2]

[1]Department of Chemistry, Yasouj University, Yasouj, Iran

[2]Department of Animal Sciences, Faculty of Agriculture, Yasouj University, Yasouj, Iran

Correspondence
M. Montazerozohori, Department of Chemistry, Yasouj University, Yasouj 7591874831, Iran.
Email: mmzohory@yahoo.com

Funding information
Yasouj University

Abstract

In this paper, five new zinc-Schiff base compounds formulated as $ZnLX_2$ (L is a new N_3-Schiff base ligand obtained by condensation reaction between diethylenetriamine and (Z)-3-(4-(dimethylamino)phenyl) acrylaldehyde and X is (Cl^-, Br^-, I^-, N_3^-, and NCS^-)) were synthesized and characterized by Fourier transform infrared, ^1H and ^{13}C NMR, UV–visible, thermal analyses, and molar conductivity measurements. Low molar conductivity values of the compounds in dimethylformamide (DMF) showed nonelectrolyte character of them. Zinc complexes have been also prepared in nanostructure sizes under ultrasonic irradiation confirmed by X-ray powder diffraction and scanning electron microscopy. Thereafter, ZnO nanoparticles were prepared by direct calcination process of zinc iodide complex at 600°C under air atmosphere. Furthermore, thermogravimetric analyses of the complexes were used for the investigation of thermal behavior of the tiled compounds. Based on TG/DTG plots, some kinetics activation parameters of the compounds at all thermal decomposition steps were calculated. In final, antimicrobial activities of the compounds were investigated by the well diffusion technique against the gram-positive bacteria of *Staphylococcus aureus* and *Bacillus subtilis*, and the gram-negative bacteria of *Escherichia coli* and *Pseudomonas aeruginosa* and the fungi strains of *Aspergillus oryzae* and *Candida albicans*. The results showed that all zinc-Schiff base organic compounds are more antimicrobial active than free ligand.

KEYWORDS

antimicrobial, nanostructure, Schiff base, thermal, zinc

1 | INTRODUCTION

The Schiff base ligand is a compound with the common structure $R_2C{=}NR'$.[1] Related to their structures, they can be considered a subclass of imines, being either secondary ketimines or secondary aldimines. Schiff bases can be prepared from an aliphatic or aromatic amine and a carbonyl compound by nucleophilic addition forming a hemiaminal, followed by a dehydration to produce an imine. The basic imine nitrogen exhibits pi acceptor properties. Conjugated Schiff bases have interesting optoelectronic properties and have been used in organic electronics such as organic solar cells,[2,3] organic field-effect transistor,[4] and electrochromic devices.[5] The simple and clean chemistry of coordination compounds make them a promising candidate as a low cost alternative to be currently used conjugated materials. Schiff base chemistry is also used to prepare covalent

organic framework, which can be used for gas storage.[6] Pharmaceutical properties of the metal complexes derived from zinc metal ion and Schiff base ligands have been widely studied, including various areas of medicinal chemistry. There are several metal complexes that are formerly in use for these purposes and this has encouraged further research on new metallodrugs such as metal-mediated antibiotics and anticancer and antiviral compounds.[7] Schiff base complexes as catalysts play an important role in a variety of chemical and photochemical reactions. In recent years, some of the chelate complexes have been used as a catalyst for solar energy storage systems. In the past two decades, Schiff bases as ligands have played a key role in the coordination chemistry of transition metals and main group metals.[8,9] These ligands are often obtained to direct synthesis routes with good yields and high purity and can easily create stable complexes with transition metal ions.[10,11] The reasons for more application of these ligands in coordination chemistry are related to electronic properties and good solubility in common solvents, easily access for their preparation and wide structural variety of these compounds.[12,13] Metal ions such as zinc (II) with enzymatic functions and its catalytic role are capable of important role in bioinorganic chemistry. Schiff base ligands also include the strong donors such as phenoxo oxygen atoms like imine nitrogen atoms, the groups that are excellent in processing the catalyst and biological activities.[14,15] Schiff base ligands are very attractive in terms of medicinal properties such as antibacterial, antiviral, antifungal, and antitumor activities.[10,11,14,16] Manganese and iron Schiff base compounds are as additive factors of resolution in MRI imaging, and because of electrical characteristics have one-dimensional and two-dimensional applications in the production of new electrical and magnetic devices.[17] The study of fluorescence properties of Schiff base compounds is very low. Some Schiff base ligands and their complexes have property of nonlinear optical, and this feature makes them to be used in optical devices.[18,19] Recently, zinc-Schiff base complexes have been used as precursor materials for synthesis of metal oxide nanoparticles. Metal oxide and/or related nanocomposite have various applications in the fields of catalyst, nanocatalyst, optoelectronic, and many others.[20–22]

Herein, in continuation of our previous reports,[23–32] synthesis and characterization of some new zinc complexes of a new tridentate Schiff base ligand entitled as (E)-N1-((E)-3-phenylallylidene)-N2-(2-((E)-((E)-3-phenylallylidene) amino) ethyl) ethane-1,2-diamine are presented. Antibacterial/antifungal properties and thermal behaviors (TG/DTG/DTA) of all zinc complexes are described. In addition, the nanostructure zinc complexes were prepared under ultrasonic irradiation. Finally, zinc complexes were used as precursors for preparation of nanostructure zinc oxide.

2 | EXPERIMENTAL

2.1 | Materials and methods

All the chemicals such as (Z)-3-(4-(dimethylamino)phenyl) acrylaldehyde (98%), diethylenetriamine(>99%), and zinc salts ($ZnCl_2$ (98%), $ZnBr_2$ (99%), ZnI_2 (99%)) were purchased from the Aldrich and/or Merck chemical companies. Zinc thiocyanate and azides were freshly prepared according to our previous report.[33] Infrared (IR) spectra were recorded by a JASCO-Fourier transform (FT)/IR-680 instrument on the range of 4000 to 400 cm^{-1} as KBr disk. ^1H and ^{13}C NMR spectra of the complexes were obtained using a Bruker DPX FT/NMR-300 spectrometer in DMSO as solvent using tetramethylsilane (TMS) as internal standard. UV–Vis spectra of the compounds in DMF were obtained from a JASCO-V570 spectrophotometer in the range of 200 to 800 nm. Kruss instrument was applied for recording of melting points or decomposition temperature (°C) of the complexes. Molar conductivity of the Schiff base ligand and their zinc complexes was determined in DMF (1.0×10^{-3} M) by a Metrohm 712 conductometer with a dip-type conductivity cell made of platinum black at room temperature. A Perkin-Elmer Pyris model Thermal gravimetric analysis (TGA) instrument was used for record of thermogravimetric diagrams. Scanning electron microscopy (SEM) images were captured on a Philips XL30 field emission scanning electron microscope using Ac voltage of 20 kV. X-ray powder diffraction (XRD) spectra were conducted on a STOE-type STIDY-MPGermany X-ray diffractometer with Cu Ka radiation (k = 1.5418 Å). The high-power ultrasonic unit Bandelin Super Sonorex RK-100H with ultrasonic peak output of 320 W and HF power of 80 Weff was handled for preparation of nanostructure complexes. In the biological tests, nutrient agar (Merck, Germany) was used as the solid medium for preparing nutrient plates, while Mueller Hinton broth (Scharlab) was used as the liquid culture media. *Escherichia coli*, *Pseudomonas aeruginosa*, *Staphylococcus aureus*, and *Bacillus subtilis* were selected for antibacterial studies and *Candida albicans* and *Aspergillus oryzae* were chosen for antifungal tests.

2.2 | Synthesis of Schiff base ligand

The Schiff base ligand was prepared according to the previous reports via a condensation reaction between 1 mmol diethylenetriamine dissolved in 5 mL of ethanol and 2 mmol of (Z)-3-(4-(dimethylamino)phenyl)

acrylaldehyde dissolved in 5 mL of ethanol under intense stirring at room temperature[33] for 5 hours. After completion of the reaction, the Schiff base was obtained as a yellow powder product. Yield: 87%. M.p.: 118–121°C.

2.3 | Synthesis of zinc complexes

Similarly, in our previous synthetic method,[27,31,33] an ethanolic solution of the fresh ligand (1 mmol) was drop by drop added to zinc halide and pseudohalide salts solution (1 mmol in 10 mL of ethanol), and the mixture was severely stirred for 4 hours at room temperature. After this time, the deposited zinc complexes were separated, washed with ethanol, and dried under air. Finally, they were identified by various techniques. Physical and spectral data (IR, UV–Visible, and NMR) of the ligand and its zinc complexes are listed in Tables 1–4.

2.4 | Synthesis of nanostructure zinc complexes

Synthesis of nanostructured zinc complexes were performed by sonochemical procedure. An ethanolic solution of the Schiff base ligand (1 mmol in 10 mL) was gradually added into zinc salts in ethanol (1 mmol in 10 mL) under ultrasonic irradiation. After addition of ligand, the reaction mixture was kept in the ultrasonic bath for 60 minutes. The nanostructured zinc complexes were collected from the solution by filtration, washed with ethanol, and dried at room temperature.

2.5 | Synthesis of zinc (II) oxide nanoparticles

A definite amount (0.7 g) of zinc iodide complex as precursor was heated to 600°C for 4 hours under air atmosphere in an electric furnace. The obtained white powder was washed with a little amount of acetone solvent and then was dried at room temperature to give zinc oxide nanoparticles in 68% yield. The ZnO nanoparticles were identified by XRD and SEM methods.

2.6 | Antimicrobial bioassay procedure

In vitro antibacterial activities of the Schiff base ligand and its zinc complexes as zone of growth inhibitory effects were surveyed by well diffusion method against gram-negative bacteria such as *E. coli* and *P. aeruginosa* and gram-positive bacteria such as *S. aureus* and *B. subtillis*. *C. albicans* and *A. oryzae* were checked as candidates for in vitro antifungal tests. For probe into the effect of concentration, ligand and its zinc complexes were dissolved in DMSO solvent. Accordingly, the stock solutions of the compounds were made in three concentrations (15, 7.5, and 3.75 mg/mL in DMSO). For DMSO against above microorganisms, no remarkable effect was reported.[27] By incubation of the microorganisms in Muller-Hinton broth medium at 37°C for 24 hours, enriched culture of them were prepared. Each sterile petri plate was treated by 15 mL of sterilized nutrient agar and Sabouraub dextrose agar for preparation of solid media for antibacterial and antifungal experiments, respectively. According to the well diffusion method, after solidification of agar gel media, 0.1 mL of suspension of mentioned microorganism was swabbed on to particular plates by a sterile glass spreader. Sterile paper disk with diameter 6 mm was loaded with a solution of compounds and located over media surface on the petri plate and afterwards they were incubated at 37°C. The diameter of the inhibition zone produced around each well was evaluated as antimicrobial activities of the newly synthesized compounds after 24 hours of incubation.

3 | RESULTS AND DISCUSSION

3.1 | Physical and analytical data

The physical properties and analytical data of the compounds have been listed in Table 1. The reaction between the tridentate Schiff base ligand (L) and ZnX_2 salts (X is Cl^-, Br^-, I^-, NCS^-, and N_3^-) in 1:1 molar ratio resulted in formation of favorable zinc complexes with the general formula of $ZnLX_2$ (Scheme 1). Solubility test of the

TABLE 1 Analytical and physical data of the Schiff base ligand and its Zn (II) complexes

Compound	Color	Dec. P., °C	Yield, %	Λ°_M, $cm^2\ \Omega^{-1}\ M^{-1}$
Ligand	Yellow	118-121 (M. P.)	87	21.7
$ZnLCl_2$	Dark orange	191-196	74	14.40
$ZnLBr_2$	Orange	241-243	86	20.4
$ZnLI_2$	Orange	243-247	85	23.0
$ZnL(SCN)_2$	Orange	234-239	78	21.6
$ZnL(N_3)_2$	Yellow	240-242	65	20.8

Abbreviations: Dec., decomposition temperature of the compound; M. P., melting point; Λ°_M, molar conductivity.

TABLE 2 Vibrational spectral data (cm^{-1}) of the Schiff base (L) and its zinc (II) complexes

Compound	ν (NH) amine	ν (CH) alkene	ν (CH) aliph.	ν (CH) imine	ν (SCN/ N3)	ν (C=N)	ν (C=C)	ν (C—N)	ν (M—N)	λ (nm), ε (M^{-1} cm
Ligand	3299	3028	2918	2881, 2803	-	1603	1460, 1442	1161	-	327 (31600), 339 (38800)
$ZnLCl_2$	3217	3037	2919	2865, 2814	-	1601	1462, 1442	1165	449	330 (7800), 385 (33000)
$ZnLBr_2$	3212	3039	2913	2867, 2815	-	1602	1484, 1442	1165	451	330 (8400), 384 (39200)
$ZnLI_2$	3205	3037	2923	2863, 2805	-	1600	1484, 1432	1167	451	330 (8400), 385 (39600)
ZnL $(SCN)_2$	3211	3041	2922	2861, 2809	2085	1593	1483, 1432	1165	453	330 (8800), 385 (40600)
ZnL $(N_3)_2$	3184	3037	2914	2865, 2815	2057	1601	1485, 1433	1165	451	331 (12600), 382 (40000)

TABLE 3 ^{1}HNMR spectral data of ligand and its zinc-Schiff base complexes in DMSO-d_6

Compound	^{1}H NMR Data (δ, ppm)
Ligand	7.97 (d, $2H_{d,d'}$, J = 9 Hz), 7.34 (d, $4H_{g,g'}$, J = 8.4 Hz), 6.92 (d, $2H_{f,f'}$, J = 15.9 Hz), 6.66 (d, $4H_{h,h'}$, J = 8.4), 6.60 (dd, $2H_{e,e'}$, J = 15.9 Hz, 9 Hz), 3.47 (t, $4H_{b,b'}$, J = 6 Hz, 4.8 Hz), 2.94 (s, $12H_{i,i'}$), 2.83 (s, $1H_a$), 2.72 (t, $4H_{c,c'}$, J = 4.8 Hz)
$ZnLCl_2$	8.13 (d, $2H_{d,d'}$, J = 6 Hz), 7.58 (dd, $2H_{e,e'}$, J = 12 Hz, 9 Hz), 7.41 (d, $4H_{g,g'}$, J = 8.4 Hz), 7.09 (bd, $2H_{f,f}$), 6.74 (d, $4H_{h,h'}$, J = 8.1), 3.60 (bt, $4H_{b,b}$), 2.97 (s, $12H_{i,i'}$), 2.86 (bt, $4H_{c,c'}$), 2.64 (bs, $1H_a$).
$ZnLBr_2$	8.23 (d, $2H_{d,d'}$, J = 8.1 Hz), 7.60 (dd, $2H_{e,e'}$, J = 9 Hz, 15 Hz), 7.41 (d, $4H_{g,g'}$, J = 7.5 Hz), 7.19 (d, $2H_{f,f'}$, J = 15 Hz), 6.74 (d, $4H_{h,h'}$, J = 6), 3.62 (bt, $4H_{b,b}$), 2.95 (s, $12H_{i,i'}$), 2.89 (t, $4H_{c,c'}$), 2.78 (bs, $1H_a$).
$ZnLI_2$	8.23 (d, $2H_{d,d'}$, J = 7.2 Hz), 7.60 (dd, $2H_{e,e'}$, J = 15 Hz, 9 Hz), 7.38 (d, $4H_{g,g'}$, J = 8.7 Hz), 7.20 (d, $2H_{f,f'}$, J = 15 Hz), 6.47 (d, $4H_{h,h'}$, J = 8.4), 3.39 (bt, $4H_{b,b}$), 3.01 (s, $12H_{i,i'}$), 2.89 (bt, $4H_{c,c'}$), 2.73 (bs, $1H_a$).
ZnL $(SCN)_2$	8.22 (d, $2H_{d,d'}$, J = 8.1 Hz), 7.62 (dd, $2H_{e,e'}$, J = 15 Hz, 8 Hz), 7.55 (d, $4H_{g,g'}$, J = 6.3 Hz), 6.64 (d, $2H_{f,f'}$, J = 15 Hz), 6.74 (d, $4H_{h,h'}$, J = 7.2), 3.54 (bt, $4H_{b,b}$), 3.00 (bt, $4H_{c,c'}$), 2.95 (s, $12H_{i,i'}$), 2.73 (bs, $1H_a$).
ZnL $(N_3)_2$	8.23 (d, $2H_{d,d'}$, J = 8.4 Hz), 7.61 (dd, $2H_{e,e'}$, J = 15 Hz, 8.4 Hz), 7.50 (d, $4H_{g,g'}$, J = 8.7 Hz), 6.75 (d, $2H_{f,f'}$, J = 15 Hz), 6.68 (d, $4H_{h,h'}$, J = 8.7), 3.56 (bt, $4H_{b,b}$), 3.00 (bt, $4H_{c,c'}$), 2.95 (s, $12H_{i,i'}$), 2.83 (bs, $1H_a$).

TABLE 4 ^{13}C NMR spectral data of ligand and its zinc-Schiff base complexes in DMSO-d_6

Compound	^{13}C NMR Data (δ, ppm)
Ligand	164.11 ($C_{3,3'}$), 151.22 ($C_{9,9'}$), 142.32 ($C_{5,5'}$), 131.12 ($C_{7,7'}$), 128.95 ($C_{6,6'}$), 123.56 ($C_{4,4'}$), 112.39 ($C_{8,8'}$), 60.89 ($C_{1,1'}$), 50.02 ($C_{2,2}$), 40.70 ($C_{10,10'}$)
$ZnLCl_2$	167.23 ($C_{3,3'}$), 154.70 ($C_{9,9'}$), 151.78 ($C_{5,5'}$), 131.12 ($C_{7,7'}$), 129.51 ($C_{6,6'}$), 123.71 ($C_{4,4'}$), 112.42 ($C_{8,8'}$), 56.37 ($C_{1,1'}$), 48.93 ($C_{2,2}$), 40.78 ($C_{10,10'}$)
$ZnLBr_2$	167.93 ($C_{3,3'}$), 154.81 ($C_{9,9'}$), 151.94 ($C_{5,5'}$), 131.13 ($C_{7,7'}$), 129.76 ($C_{6,6'}$), 123.67 ($C_{4,4'}$), 112.39 ($C_{8,8'}$), 56.28 ($C_{1,1'}$), 47.23 ($C_{2,2}$), 40.87 ($C_{10,10'}$)
$ZnLI_2$	168.50 ($C_{3,3'}$), 154.80 ($C_{9,9'}$), 152.00 ($C_{5,5'}$), 131.30 ($C_{7,7'}$), 129.90 ($C_{6,6'}$), 122.50 ($C_{4,4'}$), 112.60 ($C_{8,8'}$), 55.30 ($C_{1,1'}$), 46.50 ($C_{2,2}$), 40.80 ($C_{10,10'}$)
ZnL $(SCN)_2$	168.60 ($C_{3,3'}$), 152.00 ($C_{9,9'}$), 148.00 ($C_{5,5'}$), 133.90 (C_{NCS}), 131.30 ($C_{7,7'}$), 130.2 ($C_{6,6'}$), 122.80 ($C_{4,4'}$), 112.20 ($C_{8,8'}$), 56.80 ($C_{1,1'}$), 47.40 ($C_{2,2}$), 40.80 ($C_{10,10'}$)
ZnL $(N_3)_2$	168.10 ($C_{3,3'}$), 152.50 ($C_{9,9'}$), 151.90 ($C_{5,5'}$), 131.20 ($C_{7,7'}$), 130.00 ($C_{6,6'}$), 123.00 ($C_{4,4'}$), 112.40 ($C_{8,8'}$), 56.00 ($C_{1,1'}$), 47.80 ($C_{2,2}$), 40.50 ($C_{10,10'}$)

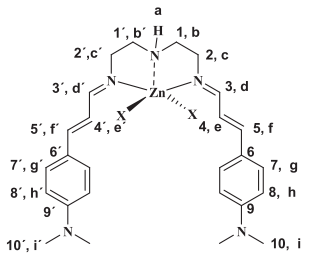

SCHEME 1 The structure of the zinc complexes

complexes and ligand in different solvents exhibited that dimethylformamide and dimethylsulfoxide are suitable solvents for them, whereas chloroform and dichloromethane dissolves slightly them. The metal complexes are nonsoluble in alcoholic media such as methanol and ethanol. All compounds are stable under air atmosphere for several months at room temperature. The ligand was obtained in 87% yields and is melted at the temperature range of 118°C to 121°C. The zinc complexes are decomposed in the temperature range of 191°C to 247°C. The yields of metal complexes were obtained in 65% to 86%. The molar conductivity values of ligand and its zinc complexes were evaluated in DMF (10^{-3} M) in the range of 14.40 to 23.00 $cm^2\ \Omega^{-1}\ mol^{-1}$ at room temperature confirming the nonelectrolytic nature of them.[34,35] The low molar conductivities indicate that the halide/pseudohalide ions and Schiff base have been bonded to zinc ion and are resistant to be dissociated in DMF solution.

3.2 | FT/IR spectra

Table 2 summarizes some selected absorption frequencies of the Schiff base ligand and its zinc complexes. In IR spectrum of ligand, the lack of bands at 1661 and 3336 cm^{-1} related to carbonyl ν (C=O) and ν (NH2) stretching vibrations (as the starting materials) and appearance of a new strong band at 1603 cm^{-1} assigned as azomethine ν (C=N) vibration indicates the formation of ligand.[25,27,36] The likely coordination sites involving in chelation are supported by the comparison of the IR spectra of the free ligand and its zinc complexes. The sharp peak appearing at 1603 cm^{-1} assigned to the azomethine vibration is shifted to lower frequencies[25,27] in the range of 1593 to 1602 cm^{-1} The weak vibrational bands at 3028, 2918, and 2881 cm^{-1} in IR spectrum of ligand are assigned to stretching vibrations of olefinic, aliphatic, and iminic C—H bonds, respectively. The movement of these signals and also the enhancement of their intensity in IR spectra of all zinc complexes well demonstrate the involvement of azomethine nitrogens in coordination to the zinc center.[26,27,30,36] The π-back bonding of metal (d^{10}) to π^* of azomethine bond of ligand may be the major reason for the wave numbers shift in the complexes spectra.[37] The broad vibrational band at the 3299 cm^{-1} observed in the spectrum of free ligand is related to N—H vibration of secondary amine group of ligand. Significant shift in vibrational frequency of secondary amine group N—H confirms the involvement of the aminic nitrogen of ligand in chelation to zinc ion. Furthermore, in complexes spectra, the appearance of the weak vibration peaks at 449 to 453 may be due to the stretching vibrations of M—N in the complexes.[25,27,36] In IR spectrum of ZnL $(NCS)_2$, vibration of the thiocyanate ligand becomes visible at 2085 cm^{-1} that shows *N*-coordination of thiocyanate ion.[34,38] The stretching vibrational frequency ν (NCS) in this compound is near to reported zinc *N*-bonded thiocyanate complexes (2077 cm^{-1}, 2073 cm^{-1}).[39–41] Finally, the appearance of a very strong and sharp peak 2057 cm^{-1} is considered as potent witness supporting the coordination of azide anions to zinc ion.[41,42]

3.3 | UV–visible spectra

The electronic spectral data of the Schiff base ligand and its zinc complexes at DMF (10^{-5} M) have been tabulated as Table 2. The electronic spectrum of ligand shows two notable absorption bands, one at 327 nm as a shoulder and the other at 339 nm, that may are considered as π–π^* intra-ligand electronic transition of phenyl rings and olefinic and azomethine bonds, respectively.[25,26,28,36] In the zinc (II) complexes electronic spectra, the first band showed no remarkable shift (3-4 nm) while the later band is shifted toward longer wavelengths that the observed red shifts attributing to elongation in the ligand conjugated system after coordination to zinc ion via azomethine nitrogens.

3.4 | NMR spectra

The NMR spectra of the Schiff base ligand and its complexes in DMSO-d_6 as solvent have been given in experimental part (Tables 3 and 4) based on Scheme 1. The ^{1}H NMR spectra of the ligand and zinc chloride complex are illustrated in Figure 1 as typical ones. In the ^{1}H NMR spectrum of the ligand, the formation of the Schiff base ligand was confirmed by appearance of the azomethine proton signal (H_d, $H_{d'}$) as a doublet with a coupling constant of 9.0 Hz at 7.97 ppm. After complexation, this signal indicates downfield shift to new position in the range of 8.13 to 8.23 ppm with a coupling constants in the range of 6.0 to 8.4 Hz that well supports change in the electron density of azomethine hydrogens after linkage to zinc ion.[23–33,43–45] The ligand spectrum shows the signals of aromatic ring protons (H_g, $H_{g'}$ and H_h, $H_{h'}$) as doublets

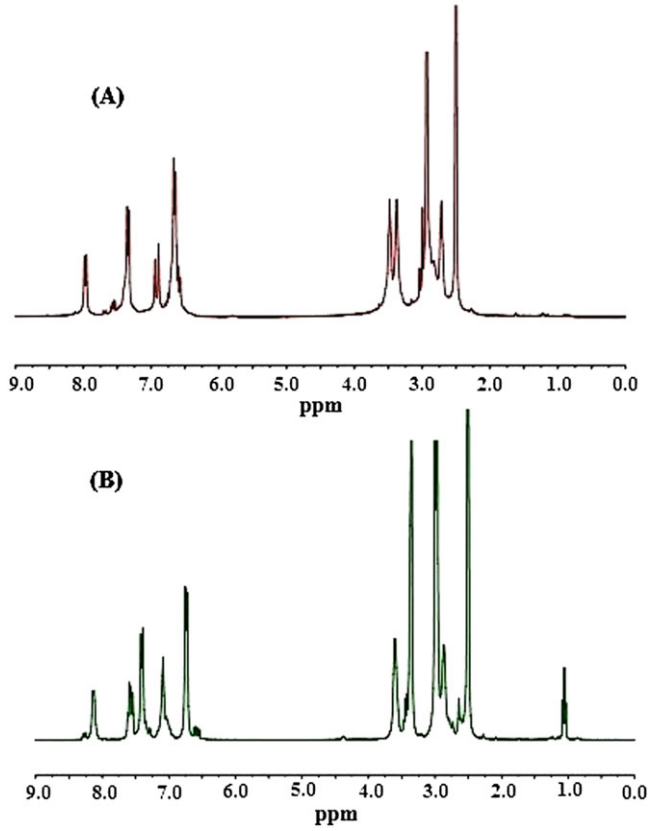

FIGURE 1 ^{1}HNMR of the A, ligand and B, zinc chloride complex

at 7.34 and 6.66 ppm with coupling constants of 8.4 and 8.4 Hz, respectively. After coordination of ligand to zinc metal ion, these signals exhibit downfield shift to new chemical shifts as shown in Table 3. In the ^{1}H NMR spectrum of Schiff base ligand, olefinic hydrogens ($H_{f,\ f'}$) observe at 6.92 ppm with a large coupling constant 15.9 Hz as a doublet due to coupling with other olefinic proton ($H_{e,\ e'}$). Based on the suggested structure for these complexes, the signal of H_f and $H_{f'}$ appeared as a doublet with coupling constant in range of 14 to 16 Hz as downfield peaks in the range of 7.09–7.20 ppm except for ZnL $(SCN)_2$ and ZnL $(N_3)_2$ complexes. Olefinic hydrogens of the ligand ($H_{e,\ e'}$), after splitting by neighboring hydrogen atoms, appear as doublet of doublet signal at 6.60 ppm. After coordination of ligand, these signals remarkably indicate downfield shift to the range of 7.58–7.62 ppm. In free ligand spectrum, aliphatic hydrogens of ($H_{b,\ b'}$) and ($H_{c,\ c'}$) appear as triplet signals in 3.47 and 2.72 ppm that after coordination of the ligand to the zinc metal ion, these signals were downfielded to 3.54 to 3.62 ppm except for $ZnLI_2$ and 2.86 to 3.00 ppm, respectively. In the ligand spectrum, aliphatic hydrogens ($H_{i,\ i'}$) appear as a singlet signal at 2.94 ppm. In all zinc complexes spectra, this signal slightly shifts to the downfield regions with respect to the free ligand. Secondary amine hydrogen in ligand spectrum appears at 2.83 ppm. This signal appears in the range of 2.64 to 2.83 ppm at the zinc complexes spectra.

In the ^{13}CNMR spectrum of the Schiff base ligand, azomethine carbon peak of ($C_{3,3'}$) appears at 164.11 ppm. This signal notably shifts to 167.23 to 168.60 ppm in its zinc complexes that is a mainspring to confirm the complex formation via azomethine nitrogen linkage to zinc ion.[23–33,43–45] The peak at 151.22 ppm attributes to ($C_{9,9'}$) that undergoes a red shift to 152.00 to 154.81 ppm in the zinc complexes spectra. According to Schiff base ligand spectrum, the signal at 142.23 ppm belongs to ($C_{5,5'}$) that shifts to 148.00 to 152.00 ppm in all complexes spectra. Based on ligand spectrum, the peak at 131.12 ppm assigns to ($C_{7,7'}$) in ligand spectrum that shifts to 134.76 to 135.36 ppm in the zinc complexes. ($C_{6,6'}$) peak appear in 128.95 ppm that shifts to the range of 129.51 to 130.2 ppm when the Schiff base ligand attach to the zinc center. The signals that appear at 123.56, 112.39, 60.89, and 50.02 ppm belonged to other free ligand carbons of ($C_{4,4'}$), ($C_{8,8'}$), ($C_{1,1'}$), and ($C_{2,2'}$), and these signals shift to the ranges of 122.50 to 123.71, 112.20 to 112.60, 55.30 to 56.80, and 46.50 to 48.93 ppm at zinc complexes spectra, respectively. In the ligand spectra, ($C_{10,10'}$) peak is found at 40.70 ppm that shifts to the range of 40.50 to 40.87 ppm when the ligand joins to the zinc ion. With respect to other complexes, an extra peak appears at 133.90 ppm in zinc thiocyanate complex dedicates to $C_{(NCS)}$. Regarding the spectral data from ^{1}H and ^{13}C NMR spectra and a comparison between peak chemical shifts in free ligand and its complexes well support the suggested structure for the zinc complexes (Scheme 1).

3.5 | XRD analysis

X-ray powder diffraction patterns of zinc chloride, iodide, thiocynate, and azide complexes prepared by the sonochemical process are represented respectively in Figure 2A-D in the 2θ range of 0°C to 90°C to evaluate the nanostructure sizes. The notable expanding of the peaks shows that the particles are of nanometer dimensions. Some 2θ angles for the zinc chloride complex are 7, 11, 13, 17, 19, 20.5, 21, 25, and 28 in degree, for the zinc iodide complex are 17, 30, and 40 in degree, for the zinc thiocyanate complex are 7.5, 17.5, 27, 28, and 42 in degree, and finally for the zinc azide complex are 6, 8, 10, 125, 18, 20, 26, and 31 in degree. The average sizes of the particles were calculated by the Scherer formula, $D = k\lambda/\beta Cos\theta$, where D is the average grain size, k is Blank's constant (0.891), λ is the X-ray wavelength (0.15405 nm), and θ and β are the diffraction angle and full-width at half maximum of an observed peak, respectively.[46] Accordingly, the average sizes of the particles

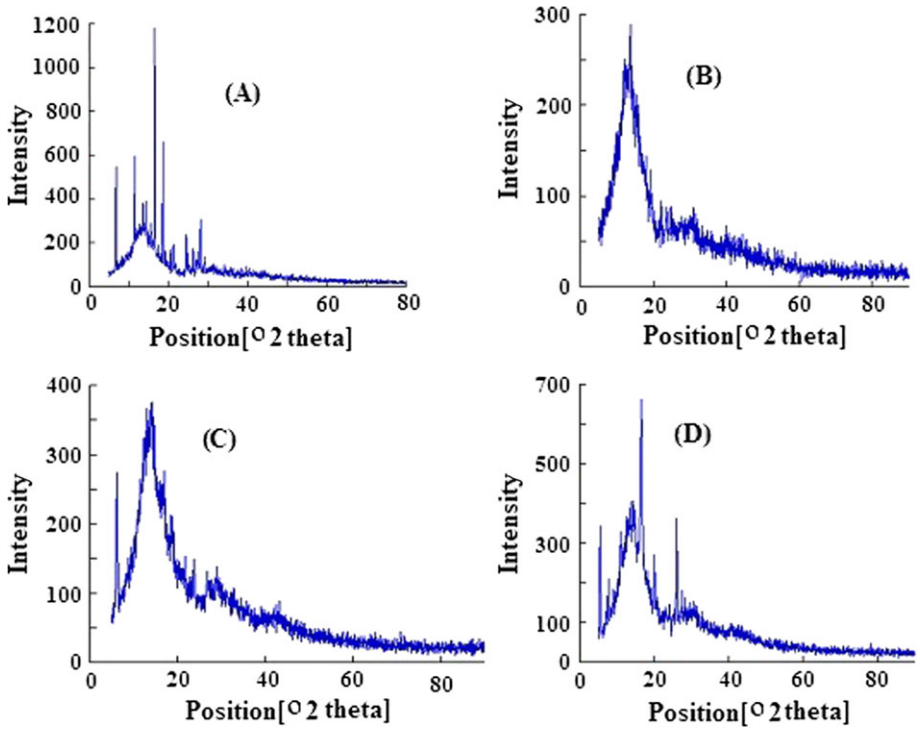

FIGURE 2 X-ray powder diffraction patterns of A, zinc chloride, B, iodide, C, thiocynate, and D, azide complexes

for zinc chloride, iodide, thiocynate, and azide were evaluated to be 62.49, 66.14, 38.37, 16.85 nm, respectively.

3.6 | SEM of the compounds

Scanning electron microscopy images of zinc (II) complexes were recorded to show the morphologies of the nanostructure complexes. From the SEM images (Figure 3), it seems that particles are well resolved. The nanoparticles are agglomerated, and a rod-like morphology is suggested for these complexes.

3.7 | Characterization of zinc oxide nanoparticles

Zinc oxide nanoparticles were prepared with direct calcination of the zinc iodide complex. After the formation, the nanoparticles were identified by XRD. The XRD pattern of zinc (II) oxide (Figure 4) is in agreement with the standard pattern of ZnO (hexagonal phase, space group $P6_3mc$, with lattice constants a = 3.2490 Å, c = 5.2050 Å, Z = 2, JCPDS card number 36-1451).[26] The XRD pattern ZnO shows that zinc oxide nanoparticles are readily prepared under mentioned synthetic conditions. Peaks for any other impurities in the XRD spectrum were not observed. The average crystallite size of ZnO nanoparticles by using the Scherer equation was obtained to be 42.81 nm.

3.8 | Thermal analyses of the zinc complexes

The thermal stability of the Schiff base and its zinc coordination complexes were investigated based on thermogravimetric method from room temperature to 900°C at a heating rate of 10°C/min under nitrogen atmosphere. The related thermal plots of complexes (TG/DTG/DTA) are demonstrated in Figure 5A-F. All thermogravimetric data including thermal decomposition steps, mass loss (%), and kinetic activation parameters of each thermal decomposition step of the ligand and its zinc complexes and final residues are listed in Tables 5 and 6. Since the TG plots indicates no weight loss below the 200°C, lack of water molecules in the complex structures is confirmed. A proposed thermal decomposition pathway for the Schiff base ligand is exhibited in Scheme 2. As suggested in Scheme 2, decomposition of the ligand is occurred in two successive steps corresponding to the elimination of the following fragments: $C_{18}H_{22}N_2$ and $C_8H_{13}N_3$. According to thermal analyses data, the zinc complexes demonstrate quite different thermal behavior. $ZnLI_2$ is destructed during two steps while $ZnLCl_2$, $ZnLBr_2$, ZnL $(NCS)_2$, and ZnL $(N_3)_2$ are decomposed thermally in three thermal steps. Zinc chloride and azide complexes are decomposed with residuals of Zn, but zinc bromide complex is completely destructed without any residual. Zinc iodide and thiocynate complexes leave out a little amount of zinc as residuals. The suggested segments eliminated from the complexes structures have been organized in Table 5.

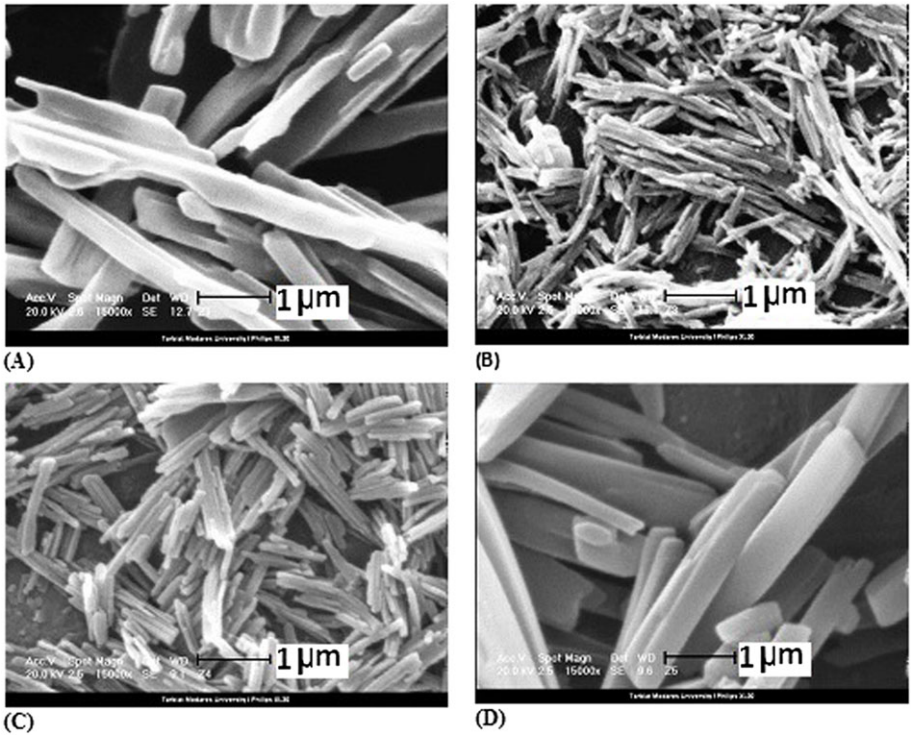

FIGURE 3 Scanning electron microscopy images of A, zinc chloride, B, iodide, C, thiocynate, and D, azide complexes

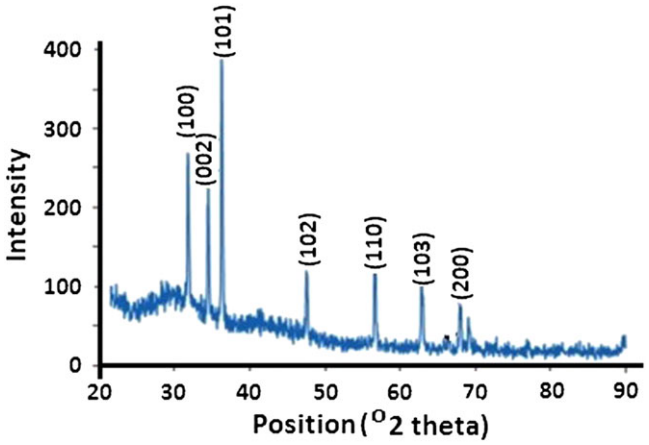

FIGURE 4 The X-ray powder diffraction pattern of ZnO nanostructure obtained from thermolysis of zinc iodide complex

Moreover, the thermodynamic activation parameters of decomposition processes of the compounds such as activation energy (ΔE*), enthalpy of activation (ΔH*), entropy of activation (ΔS*), and Gibbs free energy change (ΔG*) of the decomposition were evaluated graphically by plotting of data based on the Coats-Redfern relation[47] and tabulated in Table 6. In all complexes, the high values of activation energy propose thermal stability of the compounds within the studied temperature range.[31]

Positive value of the activation entropy (ΔS*) at the first decomposition step of $ZnLCl_2$ complex shows the dissociation nature of the process and the negative values of ΔS* for other thermal steps represent more ordered activated complex than the reactants or a slower reaction rate than normal decomposition processes.[26,48] In addition, the positive values ΔH* in the range of 11.61 to 142.12 kJ/mol reflects the endothermic character of all thermal degradation steps, and the positive values of the Gibbs free energy of activation (ΔG*) in the range of (1.25 to 3.47) × 10^2 kJ/mol reveals the nonspontaneous nature of thermal decomposition processes.

3.9 | Antibacterial bioassay (in vitro)

Biological tests of some zinc complexes by well diffusion method were evaluated for antibacterial activity against two bacteria gram-positive (*B. subtilis* and *S. aureus*) and two bacteria gram-negative (*E. coli* and *P. aeruginosa*). The collected results from experiments have been listed in Table 7 that zone diameter of inhibition from the growth (mm) are measured as antibacterial activities. According to the screening results, zinc complexes showed antimicrobial nature against various microorganisms. Generally, zinc complexes represented higher activities against microorganisms than free ligand. Based on data in Table 7, $ZnLI_2$ complex is the most effective compound against *B. subtilis* whereas ligand exhibits the weakest activity. $ZnLCl_2$ complex showed maximum activity against *S. aureus*. Other compound showed similar activity against *S. aureus*. Zinc iodide complex showed more activity against *P. aeruginosa* than ligand and other

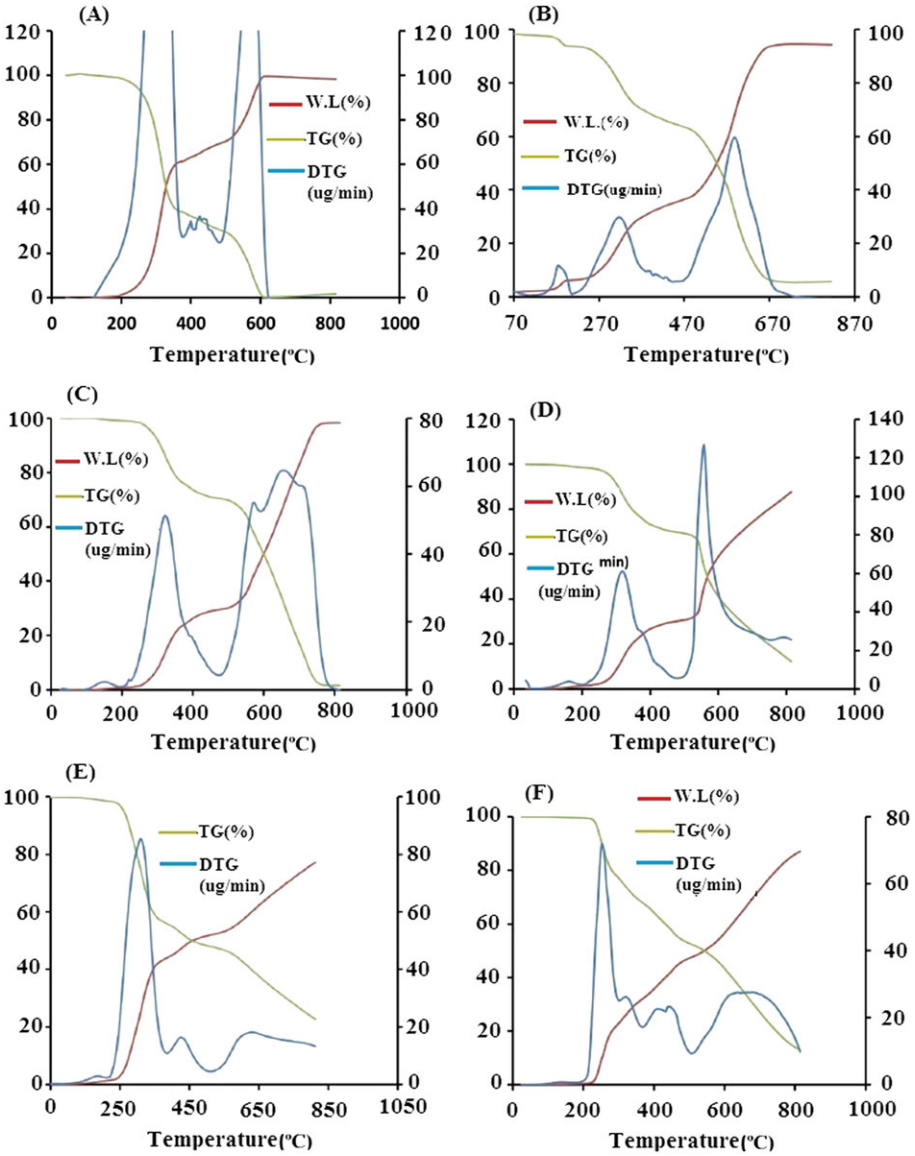

FIGURE 5 TG/DTG/DTA plots of A, ligand, B, $ZnLCl_2$, C, $ZnLBr_2$, D, $ZnLI_2$, E, ZnL $(NCS)_2$, F, and ZnL $(N_3)_2$ complexes

complexes. $ZnLCl_2$ and ZnL $(NCS)_2$ complexes have been observed to be more effective compounds against *E. coli* whereas ZnL $(N_3)_2$ had minimum bactericidal against *E. coli*. In comparison with standard drugs, the complexes showed acceptable activities against microorganisms.[36]

3.10 | Antifungal bioassay (in vitro)

Antifungal activities of the ligand and its zinc complexes were evaluated in vitro against *C. albicans* and *A. orayzea* fungal strains. The diameter of inhibition zone from the growth (mm) was measured using the well diffusion method as the antifungal activity and the bioassay results have been tabulated as Table 8. The antifungal activities data exhibited that the zinc complexes are more effective as compared with the free ligand under similar experimental conditions. Among the complexes, $ZnLI_2$ showed more inhibitory effect against *C. albicans* whereas $ZnLCl_2$ was more impressive than other complexes against *A. orayzea*. Among the complexes and the free ligand, $ZnLI_2$ complex showed higher antifungal activity against *C. albicans*. The antifungal activities of the Schiff base ligand and its zinc complexes against *A. orayzea* can be ordered as following the general trend:

$$ZnL(NCS)_2 > ZnLCl_2 > ZnLI_2 > Zn(N_3)_2 \sim \text{Ligand}.$$

According to previous reports,[26,36] the coordination of ligand to metal causes a decrease in the positive charge of zinc ion and therefore occurs π-electron delocalization on the entire complex, which leads to the biological properties of the zinc complexes that are more notable as compared with the free ligand. This results have been explained by the Overtone's concept and Tweedy's chelation theory.[49] It

TABLE 5 Thermal analysis data of the zinc complexes including temperature range, differential thermal gravimetry (DTG) peak, mass loss, proposed segment, and final residuals

Compound	Temperature Range, °C	Mass Loss Found, % (Calculated)	DTG Peak, °C	Proposed Segment	Final Residue
Ligand	190-430	65.55 (63.79)	317	$C_{18}H_{22}N_2$	-
	430-816	34.03 (36.21)	582	$C_8H_{13}N_3$	
$ZnLCl_2$	139-220	6.2 (5.43)	181	C_2H_6	Zn
	220-437	28.41 (28.93)	327	$C_{10}H_{12}N_2$	
	437-816	59.64 (59.74)	595	$C_{14}H_{17}Cl_2N_3Zn_{0.5}$	
$ZnLBr_2$	77-214	0.82 (0.93)	160	6H	-
	214-478	28.77 (28.66)	329	$C_{12}H_{12}N_2$	
	478-815	69.65 (70.40)	665	$C_{14}H_{17}Br_2N_3Zn$	
$ZnLI_2$	179-485	30.34 (29.36)	326	$C_{14}H_{20}N_2$	Zinc salt
	485-814	58.31 (58.32)	561	$C_{12}H_{15}I_{1.8}N_3$	
ZnL $(NCS)_2$	168-388	44.21 (44.46)	315	$C_{18}H_{22}N_2$	Zinc salt
	388-509	7.72 (8.69)	437	C_4H_4	
	509-813	25.36 (26.24)	633	$C_5H_9N_4S$	
ZnL $(N_3)_2$	153-373	32.26 (33.56)	256	$C_{12}H_{18}N_2$	Zn
	373-509	15.13 (15.72)	452	C_7H_5	
	509-815	39.30 (39.20)	671	$C_7H_{12}N_9$	

TABLE 6 Thermokinetic parameters of the thermal decomposition steps of the zinc complexes

Compound	Decomposition Step, °C	E*, kJ/mol	A*, 1/S	ΔS*, kJ mol K	ΔH*, kJ/mol	ΔG*, kJ/mol
Ligand	190-430	101.94	2.88×10^{6}	-1.27×10^{2}	97.03	1.72×10^{2}
	430-816	145.03	2.97	-2.45×10^{2}	137.92	3.47×10^{2}
$ZnLCl_2$	139-220	145.90	5.34×10^{14}	3.35×10^{1}	142.12	1.27×10^{2}
	220-437	51.71	5.12×10^{1}	-2.18×10^{2}	46.72	1.78×10^{2}
	437-816	93.03	7.23×10^{2}	-1.99×10^{2}	85.82	2.59×10^{2}
$ZnLBr_2$	77-214	67.79	4.20×10^{5}	-1.40×10^{2}	64.19	1.25×10^{2}
	214-478	75.24	5.35×10^{3}	-1.79×10^{2}	70.23	1.78×10^{2}
	478-815	58.46	1.83	-2.49×10^{2}	50.66	2.85×10^{2}
$ZnLI_2$	179-485	65.60	6.95×10^{2}	-1.96×10^{2}	60.61	1.78×10^{2}
	485-814	71.92	2.72×10^{1}	-2.26×10^{2}	64.99	2.53×10^{2}
ZnL $(NCS)_2$	168-388	96.43	1.01×10^{6}	-1.36×10^{2}	91.53	1.71×10^{2}
	388-509	34.46	8.33×10^{-1}	-2.54×10^{2}	28.56	2.09×10^{2}
	509-813	19.15	1.85×10^{-2}	-2.87×10^{2}	11.61	2.72×10^{2}
ZnL $(N_3)_2$	153-373	110.72	1.36×10^{8}	-9.40×10^{1}	106.32	1.56×10^{2}
	373-509	44.13	3.41	-2.42×10^{2}	38.10	2.14×10^{2}
	509-815	30.19	4.37×10^{-2}	-2.81×10^{2}	22.34	2.87×10^{2}

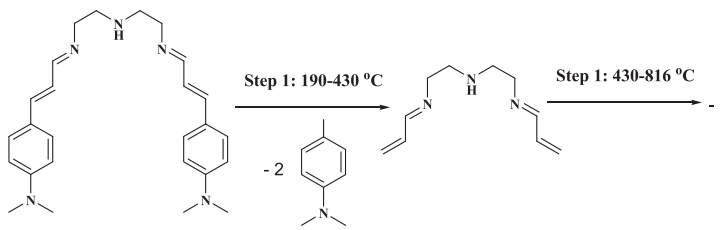

SCHEME 2 The proposed decomposition pathway for the ligand

TABLE 7 Antibacterial activity of the zinc complexes as diameter of zone of inhibition (mm) around constructed wells (saturated with 15, 7.5, and/or 3.75 mg/mL) against some bacteria

	Gram-Positive						Gram-Negative					
Compound	*Bacillus Subtilis*			*Staphylococcus Aureus*			*Pseudomonas Aeruginosa*			*Escherichia Coli*		
	15.00	7.50	3.75	15.00	7.50	3.75	15.00	7.50	3.75	15.00	7.50	3.75
Ligand	16.00	14.30	13.30	14.00	11.00	10.50	13.60	9.50	9.50	17.30	15.60	11.00
$ZnLCl_2$	24.00	16.50	11.40	16.00	14.50	11.00	12.00	11.40	10.00	20.00	15.50	13.10
$ZnLI_2$	25.60	20.00	16.60	14.40	13.40	12.00	15.50	14.00	12.00	18.00	14.50	13.80
ZnL $(NCS)_2$	19.40	19.40	19.40	14.70	13.20	12.40	13.00	15.00	12.50	20.00	17.50	16.00
ZnL $(N3)_2$	25.00	16.70	12.40	15.00	13.00	6.00	14.50	12.50	6.00	14.00	13.30	8.60

TABLE 8 Antifungal activity of the compounds as diameter of zone of inhibition (mm) around constructed disks (saturated with 15, 7.5, and/or 3.75 mg/mL) against two fungi

	Candida Albicans			*Aspergillus Orayzea*		
Compound	15	7.5	3.75	15	7.5	3.75
Ligand	16.4	14.3	13.0	6.00	6.00	6.00
$ZnLCl_2$	25.0	24.0	24.0	20.0	20.0	20.0
$ZnLI_2$	32.0	30.0	29.0	18.0	16.2	15.0
ZnL $(NCS)_2$	22.3	22.0	18.3	23.0	21.0	20.0
ZnL $(N_3)_2$	34.0	22.3	11.4	6.00	6.00	6.00

seems that the lipophilic character of the tested complexes can be a considerable factor in diffusion into cellular membrane of microorganisms. By binding the metal ion to the ligand, the lipophilicity nature of complexes is increased, that causes facilitating their passage from microorganism's cell membrane. Finally, the active site of enzyme of microorganisms is blocked by binding to the metal coordination sites and lead to preventing growth of the bacteria and/or fungi.[34,50]

4 | CONCLUSIONS

In this research, N_3-Schiff base ligand and its zinc complexes formulated as $ZnLX_2$ (L is a Schiff ligand and X is a halide or pseudohalide) were synthesized and identified by various spectral and physical techniques such as FT/IR, UV–visible, ^1H and ^{13}C NMR, thermal analyses, melting points, and molar conductivity. Also, the nanostructure forms of the zinc compounds have been prepared by the sonication process. The morphology and size of nanostructures were investigated SEM images and XRD patterns. In addition, the nanoparticles of ZnO were prepared by the calcination of $ZnLI_2$ complex at 600°C under air atmosphere that characterized by XRD. The results of thermogravimetric analysis of the ligand and its zinc complexes revealed that decomposition process happens during two to three successive thermal steps. The zinc complexes showed various thermal behaviors. The ligand and $ZnLBr_2$ were decomposed without any final residue via two and three thermal steps. $ZnLCl_2$ and $ZnLI_2$complexes lose their organic segments and Zn and a little amount of zinc salt are suggested as the residuals at final, respectively. Also ZnL $(N_3)_2$ and ZnL $(NCS)_2$ loses 86.69% and 77.29%, respectively, of their initial mass at three steps and leaving out Zn and a little amount of zinc salt at the end. The values of some thermokinetic activation parameters such as activation enthalpy (ΔH*) and Gibbs free energy (ΔG*) at all steps were positive demonstrating endothermic character for thermal decomposition of the complexes. Finally, the antimicrobial activities of the free ligand and its zinc complexes were evaluated in vitro against different bacteria and fungi. The results of antimicrobial tests revealed that the zinc complexes have higher antimicrobial activity with respect to free ligand.

ACKNOWLEDGEMENT

Partial support of this work by Yasouj University is acknowledged.

ORCID

S. Khani http://orcid.org/0000-0001-5273-2295
M. Montazerozohori http://orcid.org/0000-0001-8897-4683

REFERENCES

[1] V. Gold, K. Loening, A. McNaught and P. Shemi, *IUPAC compendium of chemical terminology*, **1997**.

[2] J. C. Hindson, B. Ulgut, R. H. Friend, N. C. Greenham, B. Norder, A. Kotlewski, T. J. Dingemans, *J. Mater. Chem.* **2010**, *20*, 937.

[3] M. Petrus, T. Bein, T. Dingemans, P. Docampo, *J. Mater. Chem. A* **2015**, *3*, 12159.

[4] D. Işık, C. Santato, S. Barik, W. Skene, *Org. Electron.* **2012**, *13*, 3022.

[5] L. Sicard, D. Navarathne, T. Skalski, W. Skene, *Adv. Funct. Mater.* **2013**, *23*, 3549.

[6] F. J. Uribe-Romo, J. R. Hunt, H. Furukawa, C. Klöck, M. O'Keeffe, O. M. Yaghi, *J. Am. Chem. Soc.* **2009**, *131*, 4570.

[7] R. Shanmugakala, P. Tharmaraj, C. Sheela, N. Chidambaranathan, *Med. Chem. Res.* **2014**, *23*, 329.

[8] S. Abdel-Latif, H. Hassib, Y. Issa, *Spectrochim. Acta, Part a* **2007**, *67*, 950.

[9] S. Meghdadi, M. Amirnasr, K. Mereiter, A. Amiri, V. Ghodsi, *Inorg. Chim. Acta* **2010**, *363*, 1587.

[10] G. G. Mohamed, M. Zayed, S. Abdallah, *J. Mol. Struct.* **2010**, *979*, 62.

[11] S. Nayak, P. Gamez, B. Kozlevčar, A. Pevec, O. Roubeau, S. Dehnen, J. Reedijk, *Polyhedron* **2010**, *29*, 2291.

[12] G. Bhargavi, M. Rajasekharan, J.-P. Costes, J.-P. Tuchagues, *Polyhedron* **2009**, *28*, 1253.

[13] K. Gupta, A. K. Sutar, *Coord. Chem. Rev.* **2008**, *252*, 1420.

[14] S. Basak, S. Sen, S. Banerjee, S. Mitra, G. Rosair, M. G. Rodriguez, *Polyhedron* **2007**, *26*, 5104.

[15] H. Khanmohammadi, S. Amani, M. H. Abnosi, H. R. Khavasi, *Spectrochim. Acta, Part a* **2010**, *77*, 342.

[16] T. Rosu, E. Pahontu, C. Maxim, R. Georgescu, N. Stanica, G. L. Almajan, A. Gulea, *Polyhedron* **2010**, *29*, 757.

[17] F. A. Mautner, A. Egger, B. Sodin, M. A. Goher, M. A. Abu-Youssef, A. Escuer, R. Vicente, *J. Mol. Struct.* **2010**, *969*, 192.

[18] C.-G. Liu, Y.-Q. Qiu, S.-L. Sun, N. Li, G.-C. Yang, Z.-M. Su, *Chem. Phys. Lett.* **2007**, *443*, 163.

[19] C.-G. Liu, Y.-Q. Qiu, S.-L. Sun, H. Chen, N. Li, Z.-M. Su, *Chem. Phys. Lett.* **2006**, *429*, 570.

[20] M. H. Habibi, M. Fakhrpor, *J. Mater. Sci.: Mater. Electron.* **2017**, *28*, 2697.

[21] M. H. Habibi, M. Mardani, M. Habibi, M. Zendehdel, *J. Mater. Sci.: Mater. Electron.* **2017**, *28*, 3789.

[22] M. H. Habibi, M. Mardani, *J. Mol. Liq.* **2017**, *238*, 397.

[23] S. G. Niyaky, M. Montazerozohori, A. Masoudiasl, J. White, *J. Mol. Struct.* **2017**, *1131*, 201.

[24] M. Montazerozohori, A. Masoudiasl, T. Doert, *Inorg. Chim. Acta* **2016**, *443*, 207.

[25] M. Montazerozohori, S. Musavi, A. Masoudiasl, A. Naghiha, M. Dusek, M. Kucerakova, *Spectrochim. Acta, Part a* **2015**, *137*, 389.

[26] A. Masoudiasl, M. Montazerozohori, R. Naghiha, A. Assoud, P. McArdle, M. S. Shalamzari, *Mater. Sci. Eng., C* **2016**, *61*, 809.

[27] M. Montazerozohori, S. M. Jahromi, A. Naghiha, *J. Ind. Eng. Chem.* **2015**, *22*, 248.

[28] M. Montazerozohori, S. A. Musavi, *J. Coord. Chem.* **2008**, *61*, 3934.

[29] M. Montazerozohori, S. Yadegari, A. Naghiha, S. Veyseh, *J. Ind. Eng. Chem.* **2014**, *20*, 118.

[30] M. Montazerozohori, S. Zahedi, A. Naghiha, M. M. Zohour, *Mater. Sci. Eng., C* **2014**, *35*, 195.

[31] M. Montazerozohori, S. A. Musavi, A. Naghiha, M. M. Zohour, *Spectrochim. Acta, Part a* **2014**, *129*, 382.

[32] M. Montazerozohori, S. A. Musavi, A. Naghiha, S. Veyseh, *Journal of Chemical Sciences* **2014**, *126*, 227.

[33] M. Montazerozohori, S. Khani, H. Tavakol, A. Hojjati, M. Kazemi, *Spectrochim. Acta, Part a* **2011**, *81*, 122.

[34] A. D. Kulkarni, S. A. Patil, P. S. Badami, *Int. J. Electrochem. Sci.* **2009**, *4*, 717.

[35] M.-H. E. Chan, K. A. Crouse, M. I. M. Tahir, R. Rosli, N. Umar-Tsafe, A. R. Cowley, *Polyhedron* **2008**, *27*, 1141.

[36] M. Montazerozohori, S. M. Jahromi, A. Masoudiasl, P. McArdle, *Spectrochim. Acta, Part a* **2015**, *138*, 517.

[37] N. Dharmaraj, P. Viswanathamurthi, K. Natarajan, *Transition Met. Chem.* **2001**, *26*, 105.

[38] M. P. Gashti, M. Bourquin, M. Stir, J. Hulliger, *J. Mater. Chem. B* **2013**, *1*, 1501.

[39] M. Đaković, Z. Popović, G. Giester, M. Rajić-Linarić, *Polyhedron* **2008**, *27*, 210.

[40] P. Bhowmik, S. Chattopadhyay, M. G. Drew, C. Diaz, A. Ghosh, *Polyhedron* **2010**, *29*, 2637.

[41] B. Samanta, J. Chakraborty, C. Choudhury, S. Dey, D. Dey, S. Batten, P. Jensen, G. P. Yap, S. Mitra, *Struct. Chem.* **2007**, *18*, 33.

[42] M. A. Goher, F. A. Mautner, B. Sodin, B. Bitschnau, *J. Mol. Struct.* **2008**, *879*, 96.

[43] Z. H. Chohan, *Transition Met. Chem.* **2009**, *34*, 153.

[44] G. Consiglio, I. Pietro Oliveri, S. Failla, S. Di Bella, *Inorganics* **2018**, *6*(8), 1.

[45] F. Chioma, A. C. Ekennia, A. A. Osowole, S. N. Okafor, C. U. Ibeji, D. C. Onwudiwe, O. T. Ujam, *Open Chemistry* **2018**, *16*, 184.

[46] J. Yang, C. Lin, Z. Wang, J. Lin, *Inorg. Chem.* **2006**, *45*, 8973.

[47] A. W. Coats, J. Redfern, *Nature* **1964**, *201*, 68.

[48] J. W. Moore, R. G. Pearson, *Kinetics and mechanism*, John Wiley & Sons **1961**.

[49] B. Tweedy, *Phytopathology* **1964**, *55*, 910.

[50] A. Kulkarni, S. A. Patil, P. S. Badami, *Eur. J. Med. Chem.* **2009**, *44*, 2904.

How to cite this article: Khani S, Montazerozohori M, Naghiha R. Some novel nanostructure Schiff base compounds: Antimicrobial and thermal behaviors. *J Phys Org Chem*. 2018;e3873. https://doi.org/10.1002/poc.3873